Pheromone routing protocol on a scale-free network

Xiang Ling,[1] Mao-Bin Hu,[1,*] Rui Jiang,[1,†] Ruili Wang,[2] Xian-Bin Cao,[3] and Qing-Song Wu[1]

[1]*School of Engineering Science, University of Science and Technology of China, Hefei 230026, People's Republic of China*
[2]*School of Engineering and Advanced Technology, Massey University, Turitea, Palmerston North 4442, New Zealand*
[3]*Department of Computer Science and Technology, University of Science and Technology of China,*
Hefei 230026, People's Republic of China

This paper proposes a routing strategy for network systems based on the local information of "pheromone." The overall traffic capacity of a network system can be evaluated by the critical packet generating rate R_c. Under this critical generating rate, the total packet number in the system first increases and then decreases to reach a balance state. The system behaves differently from that with a local routing strategy based on the node degree or shortest path routing strategy. Moreover, the pheromone routing strategy performs much better than the local routing strategy, which is demonstrated by a larger value of the critical generating rate. This protocol can be an alternation for superlarge networks, in which the global topology may not be available.

I. INTRODUCTION

Complex networks can describe many natural and social systems in which entities or people are connected by physical links or some abstract relationship. Since the discovery of the small-world phenomenon [1], and scale-free property [2], complex networks have attracted growing interest among the community of physicists [3–6].

The traffic is one of the hot topics of recent research of dynamical processes taking place in complex network systems. In the past few years, the phase transition in network traffic [7–10], the scaling of traffic fluctuations [11–14], and the routing strategies (including global and local information routing [15–32]) have been widely studied. Our focus here is the routing strategy for networked systems, such as the Internet, urban traffic, airway system, and power grids. For modern networked systems, one important problem is to find an efficient routing strategy in a growing superlarge system without knowing the whole topological information. The shortest path strategy, however, often leads to the failure of hub routers with high degree and high betweenness. In this light, some new routing strategies have been suggested based on the local topological information. For example, Wang *et al.* [30] and Yin *et al.* [31] proposed a local routing strategy based on the local information of neighbors' degree. Hu *et al.* proposed a local routing strategy based on the local information of link bandwidth [32].

Recently, the study of ant colonies, swarm intelligence, and trails have become a hot topic [33–37]. The ant colony algorithm is a good method for achieving a best solution for the traffic problem [38].

In this paper, we propose a routing strategy based on the local information of pheromone. In biology, pheromone is a chemical released by an animal to give information to other family members. Pheromone is believed to be an important chemical signal for the guidance of following ants to find the correct path from the nest to the food [36]. In their paper [36], Colorni *et al.* studied the behavior of ant colonies, in which all ants only communicated with their neighbors. In the process of moving, the ants will release a special kind of secretion pheromone which helps other ants to look for a path. The ants choose a path i with the probability of $P_i = \rho_i / \Sigma_j \rho_j$, where ρ_i is the concentration of pheromone in path i and the sum runs over the paths. For a path, the more ants select it, the more pheromone will be left in this path. The larger concentration of pheromone will attract more ants, thus producing a positive feedback mechanism. So the concentration of pheromone on the optimal path will increase, while other path's pheromone will decrease until disappear.

In this paper, we extend the ant colony algorithm to scale-free networks and study the behavior of the traffic dynamics. We focus on the network capacity that can be measured by the critical point of phase transition from free flow to congestion. In our model, there is only one adjustable parameter α. Numerical simulations have demonstrated that the system behaves differently from the other strategies. We also find that the maximal capacity corresponds to $\alpha = 1.0$ in the case of identical nodes' delivering ability. Most importantly, the system's overall capacity is much higher than that with a routing strategy based on local degree or bandwidth information.

The paper is organized as follows. In the next section, the underlying network model and the traffic model are introduced. Section III gives the simulation results of our pheromone routing strategy. The paper is concluded in Sec. IV.

II. NETWORK AND TRAFFIC MODEL

Recent studies indicate that many communication systems such as the Internet and the World Wide Web are not homogeneous as random or regular networks, but heterogeneous with degree distribution following the power-law distribution $P(k) = k^{-\gamma}$. The Barabási-Albert (BA) model [2] is a well-known model which can generate networks with power-law degree distribution. Without lose of generality, we construct the underlying network structure with the BA network
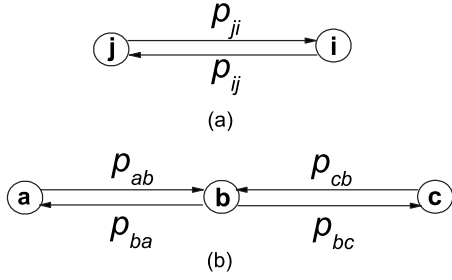
———————
*humaobin@ustc.edu.cn
†rjiang@ustc.edu.cn

FIG. 1. (a) The pheromone of links ij and ji. Generally, $p_{ji} \neq p_{ij}$. (b) The pheromone of a node is defined as the sum of pheromone of links going toward the node. For example, the pheromone of node b is $p_b = p_{ab} + p_{cb}$.

model: starting from m_0 fully connected nodes, a new node with m ($m \leq m_0$) edges is added to the existing graph at each time step according to preferential attachment, i.e., the probability Π_i of being connected to the existing node i is proportional to the degree k_i of the existing node. In this paper, we set $m_0 = m = 5$ and the network size $N = 1000$.

The traffic model is described as follows. At each time step, there are R packets generated in the system, with randomly chosen sources and destinations. One node can deliver at most C (in this paper we set $C = 1$) packets to its neighboring nodes. The packets are delivered by the local information of pheromone, which is defined on the links. In every time step, each node performs a local search among its neighbors. If a packet's destination is found within the searched area, it is delivered directly to its target. Otherwise, the packet is delivered to a neighboring node j with probability

$$P_{i \to j} = \frac{p_{ij}^{\alpha}}{\sum\limits_{j} p_{ij}^{\alpha}}, \qquad (1)$$

where p_{ij} is the pheromone of the link pointing from node i to node j, the sum runs over all neighbors of node i, and α is a tunable parameter characterizing the routing preference. Note that p_{ij} can be different from p_{ji}, as shown in Fig. 1(a). Once arriving at its destination, the packet will be removed from the system. The queue length of each node is assumed to be unlimited and the first in first out rule is applied to all queues.

Next we introduce the updating rule for the pheromone of a link. Initially, the value of the pheromone concentration on each link is set to a small unit value of δp. The pheromone of each link cannot be smaller than this value δp. Whenever a packet is delivered successfully from node i to node j, the pheromone of link ij will be updated according to the following rule: if the queue length of node j is larger than a critical value, i.e., $L_j > L_c$, the pheromone of link ij will decrease by a unit,

$$p_{ij} = \max\{p_{ij} - \delta p, \delta p\}. \qquad (2)$$

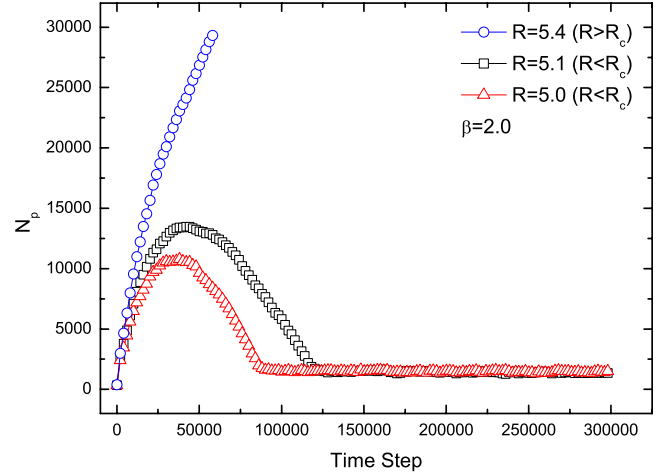Otherwise, if the queue length $L_j \leq L_c$, the pheromone will increase by a unit value,

FIG. 2. (Color online) Typical variation of N_p for the pheromone routing strategy in the free-flow ($R < R_c$) and jam ($R > R_c$) states. The parameters are $\alpha = 1.0$ and $\beta = 2.0$.

$$p_{ij} = p_{ij} + \delta p. \qquad (3)$$

In this paper, we set the unit value as $\delta p = 0.001$. The critical queue length is set to be proportional to the delivery ability of the node: $L_c = \beta C$. Then we investigate the effects of α and β on the traffic dynamics of the system.

III. SIMULATION RESULTS

In this section, we show the simulation results of the pheromone routing strategy on a BA scale-free network. Figure 2 shows the typical evolution of total packets number N_p over time with the pheromone routing strategy. When R is smaller than a critical value R_c (R_c characterizes the overall capacity of the system, which will be introduced later), one can see that the variation of N_p can be divided into two stages: the relaxation and balanced stages. In the relaxation stage, N_p first increases to a maximum and then decreases to a balanced state. In the balanced stage, N_p is almost constant, indicating that the numbers of generated and removed packets are balanced. When R is larger than the critical value of R_c, N_p increases to infinity, indicating that the system enters a jam state.

In the relaxation stage, the concentration of pheromone is automatically adjusted to achieve an optimal state. One can investigate the normalized average node pheromone $\langle p_k \rangle$ as a function of node degree k. A node's pheromone is defined as the sum of the link pheromone going toward the node, as shown in Fig. 1(b). The normalized average node pheromone is calculated by

$$\text{Normalized } \langle p_k \rangle = \frac{\langle p_k \rangle}{\langle p_k^{max} \rangle}, \qquad (4)$$

with

$$\langle p_k \rangle = \frac{\Sigma p_{(\text{degree} = k)}}{\text{Number } (\text{degree} = k)}. \qquad (5)$$

Figure 3 shows the normalized pheromone $\langle p_k \rangle$ for different evolution times for the system. In both the increasing and
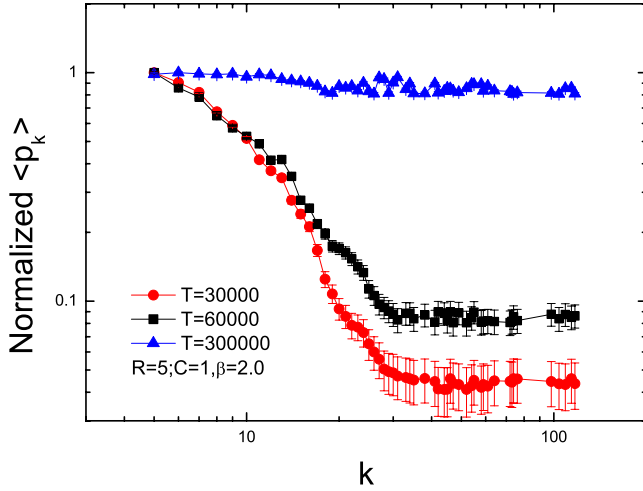
FIG. 3. (Color online) The normalized average node pheromone $\langle p_k \rangle$ at different times. Other parameters are $R=5$, $C=1$, $\alpha=1.0$, and $\beta=2.0$.

decreasing periods of the relaxation stage ($T=30\,000$ and $60\,000$), the normalized pheromone $\langle p_k \rangle$ follows a power law. The average pheromone of low-degree nodes are higher than that of high-degree nodes. Because the hub nodes bear more traffic load, the node pheromone decreases according to Eq. (2). On the other hand, in the balanced stage ($T=300\,000$), the normalized pheromone $\langle p_k \rangle$ is almost independent of k. At this point, the hub nodes have roughly the same pheromone as the low-degree nodes. Thus, the pheromone of the links going to hub nodes are much lower than that of the links going to low-degree nodes. According to the delivering rule, the packets are encouraged to go to low-degree nodes. However, because the hub nodes have more links, the total delivering probabilities of going to hub nodes and low-degree nodes are similar. The ability of both hub nodes and low-degree nodes can be fully utilized. Thus, the system achieves its optimum.

Figure 4 shows the relaxation stage of N_p with different values of β. One can see that the behavior of N_p is similar for
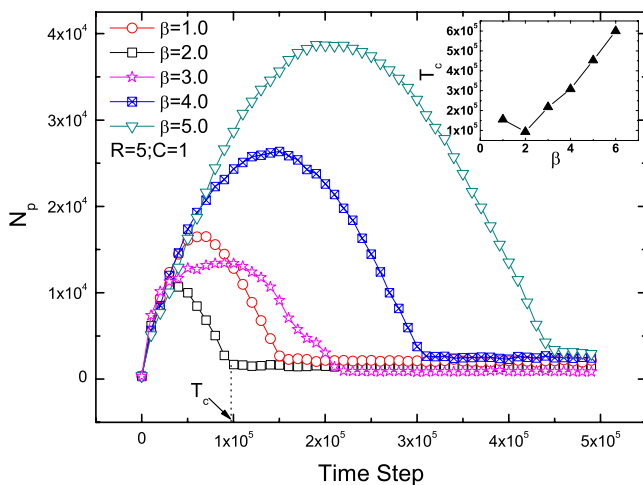

FIG. 4. (Color online) The variation of N_p with different β. The inset shows T_c with different β.
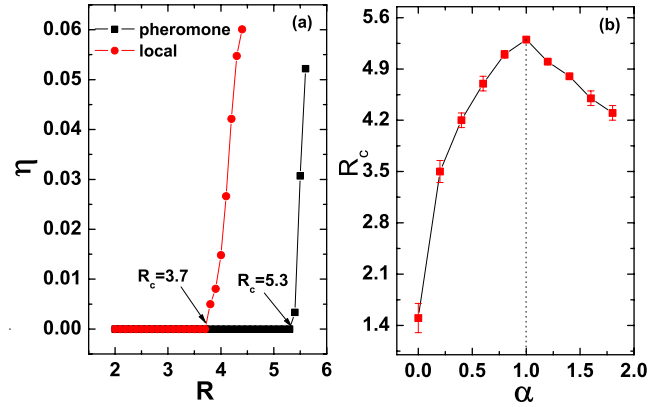

FIG. 5. (Color online) (a) The order parameter η as a function of generating rate R for pheromone routing strategy and local degree routing strategy. The routing parameter is set to $\alpha=1.0$ for the pheromone routing strategy and $\alpha=-1.0$ for the local routing strategy. Other parameters are $N=1000$, $m_0=m=5$, $C=1$, and $\beta=2.0$ for the pheromone routing strategy. (b) R_c versus α with constant node capacity $C=1$. The maximum of R_c corresponds to $\alpha=1.0$ marked by a dotted line.

different β. One important issue here is to figure out the optimal value of β, at which the relaxation stage will be shortest for the system. We can investigate the critical time T_c at which N_p reaches the balanced stage. Figure 6 inset shows T_c with different values of β. When $\beta=2$, T_c reaches its minimum. Thus, we can see that $\beta=2$ is the optimum for the system to quickly reach the balanced state.

In order to describe the phase transition of traffic flow in the network, we adopt the order parameter [7]

$$\eta(R) = \lim_{t \to \infty} \frac{C}{R} \frac{\langle \Delta N_p \rangle}{\Delta t}, \qquad (6)$$

where $\Delta N_p = N_p(t+\Delta t) - N_p(t)$ and $\langle \cdots \rangle$ indicates the average over time windows of width Δt. In Fig. 5(a), the typical variation of η against R is shown for the pheromone routing strategy and the local routing strategy. The pheromone routing strategy is with parameter $\alpha=1.0$, at which we will demonstrate that the maximum overall capacity is achieved. The local routing strategy [30] is with the parameter of $\alpha=-1.0$, at which the maximum capacity is reached. For $R<R_c$, η remains at zero, indicating that the system is in the free-flow state. With the increase in packet generation rate R, there will be a critical value of R_c at which η increases from zero, indicating that the packets accumulate in the system, and the system becomes seriously congested [7]. Therefore, R_c is the maximal generating rate under which the system can maintain its normal and efficient functioning. One can see that the pheromone routing strategy can reach a larger network capacity. As shown in Fig. 5(a), the maximal overall capacity is $R_c=3.7$ with local degree routing strategy, while it is $R_c=5.3$ for the local pheromone routing strategy. In Fig. 5(b), the overall capacity R_c is sought out for different values of routing parameter α with constant node capacity $C=1$. One can see that, when $\alpha=1.0$, the system's capacity can be enhanced maximally.
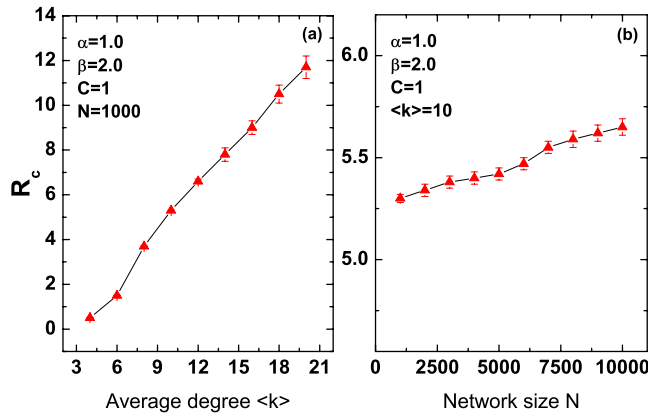
FIG. 6. (Color online) (a) Network capacity R_c vs average degree $\langle k \rangle$ with the same network size of $N=1000$. (b) Network capacity R_c vs network size N with the same average degree of $\langle k \rangle =10$. Other parameters are $C=1$, $\alpha=1.0$, and $\beta=2.0$ for both situations.

We also investigated the effects of average node degree $\langle k \rangle$ and network size N on the traffic capacity of network, as shown in Fig. 6. In Fig. 6(a), one can see that R_c increases almost linearly with the increase in average degree $\langle k \rangle$ and in Fig. 6(b), R_c also increase slightly with the increase in network size.

To better understand why $\alpha=1.0$ is the optimal value, we investigate the average packet number $n(k)$ of nodes as a function of its degree k in the balanced stage, as shown in Fig. 7. The average is over the nodes with the same degree. When $\alpha<1.0$ [Figs. 7(a) and 7(b)], although the value of $n(k)$ remains around 1.0, the distribution of $n(k)$ follows a power law of $n(k) \sim k^\gamma$ with exponent $\gamma>0$. This indicates that the high-degree nodes are slightly overburdened. Since all nodes have the same delivering ability, this phenomenon will harm the system capacity. When $\alpha=1.0$ [Fig. 7(c)], $n(k)$ is independent of k. The traffic load is homogeneously distributed among the nodes and thus lead to a maximum R_c.
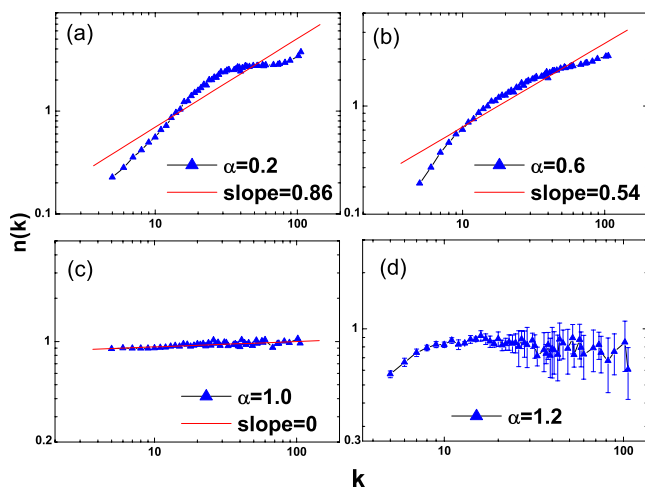

FIG. 7. (Color online) Average packet number for nodes $n(k)$ depending on degree k for different α in balanced stage. The error bars in (d) show the fluctuations in the value of $n(k)$. Other parameters are $R=3<R_c$, $C=1$, and $\beta=2.0$.
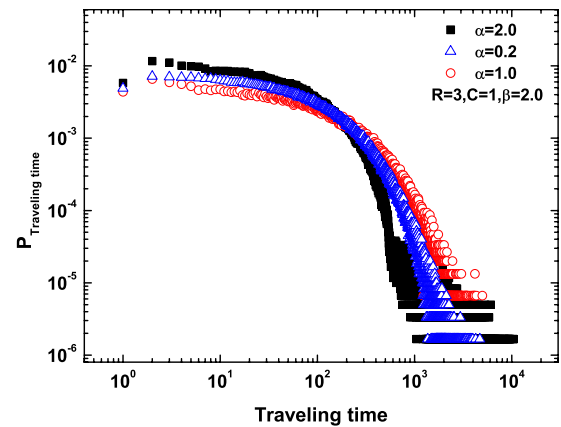

FIG. 8. (Color online) The probability distribution of traveling time for different α.

When $\alpha>1.0$ [Fig. 7(d)], there are obvious fluctuations in the value of $n(k)$, especially for large-degree nodes. We also investigate the situations of bigger α value. The fluctuations of $n(k)$ are more evident. Therefore, it is easier for the hub nodes to get congested when $\alpha>1.0$. So the system capacity decreases.

Then we investigate the probability distribution of traveling time for different α in a free-flow state. Packet traveling time is also an important factor for characterizing the network's behavior. The traveling time is the time that a packet spends on traveling from a source to a destination. In Fig. 8, one can see that the distribution of traveling time follows a subpower law. Most packets can arrive at their destinations in a short time while some packets need to spend very long time to find their target nodes. We also note that, when $\alpha=1.0$, the packets spend the shortest time for traveling. This is consistent with the result of Fig. 6 that the network's capacity reached a maximum when $\alpha=1.0$.

Finally, we briefly introduce the effect of node delivering ability C on the traffic dynamics. The qualitative behavior is not affected by varying C. In general, the system's overall capacity will increase with the increase in C, and the optimal value of α_c remains the same.

We also apply the pheromone routing strategy in Erdos-Renyi and Watts-Strogatz networks [1]. The former provides a uniformly random reference, while the latter accounts for several types of real-world networks. However, the improvement in network capacity is not so obvious in these two networks. The pheromone routing strategy can perform better in a heterogeneous network than in a homogeneous network.

IV. CONCLUSION AND DISCUSSION

In summary, we have proposed a routing protocol for a modern traffic system based on the local information of pheromone and then investigated the behavior of the traffic system. The system performs better under the pheromone routing strategy than under the local routing strategy by node degree or link bandwidth. Due to the difficulty of obtaining the information of the whole network's topology in modern

communication and traffic systems, the routing protocols based on the local information are attracting much interest [30–32]. The pheromone routing strategy performs best among the routing protocols of local information. This is a nontrivial improvement in the network traffic area.

In the model, the traffic system automatically adjust the distribution of pheromone to achieve a balanced state. In the balanced state, the traffic load will be homogeneously distributed among the nodes. The relaxation process depends on the traffic parameter. The optimal value of pheromone updating parameter β should be set to $\beta=2.0$, at which the relaxation process will be minimal. Simulations have shown that the optimal routing strategy should be set to $\alpha=1.0$, which is different from the local routing strategy [30]. The distribution of traveling time is also investigated. These phenomena are unique and can trigger more interest in this field. The model can be useful for the design and optimization of routing strategies in some real traffic systems such as the urban transportation systems, peer-to-peer networks, wireless sensor networks, and so on.

[1] D. J. Watts and S. H. Strogatz, Nature (London) **393**, 440 (1998).

[2] A.-L. Barabási and R. Albert, Science **286**, 509 (1999).

[3] R. Albert and A.-L. Barabási, Rev. Mod. Phys. **74**, 47 (2002).

[4] M. E. J. Newman, Phys. Rev. E **64**, 016132 (2001).

[5] M. E. J. Newman, SIAM Rev. **45**, 167 (2003).

[6] S. Boccaletti *et al.*, Phys. Rep. **424**, 175 (2006).

[7] A. Arenas, A. Díaz-Guilera, and R. Guimerá, Phys. Rev. Lett. **86**, 3196 (2001).

[8] T. Ohira and R. Sawatari, Phys. Rev. E **58**, 193 (1998).

[9] D. De Martino, L. Dall'Asta, G. Bianconi, and M. Marsili, Phys. Rev. E **79**, 015101(R) (2009).

[10] R. V. Solé and S. Valverde, Physica A **289**, 595 (2001).

[11] M. A. de Menezes and A.-L. Barabási, Phys. Rev. Lett. **92**, 028701 (2004).

[12] S. Meloni, J. Gómez-Gardeñes, V. Latora, and Y. Moreno, Phys. Rev. Lett. **100**, 208701 (2008).

[13] J. Duch and A. Arenas, Phys. Rev. Lett. **96**, 218702 (2006).

[14] Z. Eisler, J. Kertesz, S.-H. Yook, and A.-L. Barabási, EPL **69**, 664 (2005).

[15] Petter Holme and Beom Jun Kim, Phys. Rev. E **65**, 066109 (2002).

[16] L. Zhao, K. Park, and Y. C. Lai, Phys. Rev. E **70**, 035101(R) (2004).

[17] L. Zhao, Y.-C. Lai, K. Park, and N. Ye, Phys. Rev. E **71**, 026125 (2005).

[18] R. Guimerà, A. Díaz-Guilera, F. Vega-Redondo, A. Cabrales, and A. Arenas, Phys. Rev. Lett. **89**, 248701 (2002).

[19] R. Guimerà, A. Arenas, A. Díaz-Guilera, and F. Giralt, Phys. Rev. E **66**, 026704 (2002).

[20] G. Yan, T. Zhou, B. Hu, Z. Q. Fu, and B. H. Wang, Phys. Rev. E **73**, 046108 (2006).

[21] B. Danila, Y. Yu, J. A. Marsh, and K. E. Bassler, Phys. Rev. E **74**, 046106 (2006).

[22] X. Ling, R. Jiang, X. Wang, M. B. Hu, and Q. S. Wu, Physica A **387**, 4709 (2008).

[23] J. M. Kleinberg, Nature (London) **406**, 845 (2000).

[24] B. J. Kim, C. N. Yoon, S. K. Han, and H. Jeong, Phys. Rev. E **65**, 027103 (2002).

[25] L. A. Adamic, R. M. Lukose, A. R. Puniyani, and B. A. Huberman, Phys. Rev. E **64**, 046135 (2001).

[26] Carlos P. Herrero, Phys. Rev. E **71**, 016103 (2005).

[27] Shi-Jie Yang, Phys. Rev. E **71**, 016107 (2005).

[28] B. Tadić, S. Thurner, and G. J. Rodgers, Phys. Rev. E **69**, 036102 (2004).

[29] A. T. Lawniczak and X. Tang, Eur. Phys. J. B **50**, 231 (2006).

[30] W. X. Wang, B. H. Wang, C. Y. Yin, Y. B. Xie, and T. Zhou, Phys. Rev. E **73**, 026111 (2006).

[31] C. Y. Yin, B. H. Wang, W. X. Wang, T. Zhou, and H. Yang, Phys. Lett. A **351**, 220 (2006).

[32] M. B. Hu, W. X. Wang, R. Jiang, Q. S. Wu, and Y. H. Wu, EPL **79**, 14003 (2007).

[33] J. A. Pimentel, M. Aldana, Cristián Huepe, and Hernán Larralde, Phys. Rev. E **77**, 061138 (2008).

[34] K. Nishinari, D. Chowdhury, and A. Schadschneider, Phys. Rev. E **67**, 036120 (2003).

[35] A. John, A. Schadschneider, D. Chowdhury, and K. Nishinari, Phys. Rev. Lett. **102**, 108001 (2009).

[36] A. Colorni, M. Dorigo, and V. Maniezzo, in *Proceedings of the First European Conference on Artificial Life, Paris, 1991*, edited by F. Varela and P. Bourgine (Elsevier, Paris, 1991), pp. 134–142.

[37] L. da Fontoura Costa, F. A. Rodrigues, and G. Travieso, Phys. Rev. E **76**, 046106 (2007).

[38] E. Bonabeau, M. Dorigo, and G. Theraulaz, Nature (London) **406**, 39 (2000).